Ab Initio Spin−Orbit Configuration Interaction Calculations for High-Lying States of the HeNe Quasimolecule

Robert J. Buenker,[†,*] Heinz-Peter Liebermann,[†] and Alexander Z. Devdariani[†,‡]

Fachbereich C-Mathematik und Naturwissenschaften, Bergische Universitaet Wuppertal, Gaussstrasse 20, D-42119 Wuppertal, Germany, and Institute of Physics, St. Petersburg University, Peterhof, St. Petersburg, 198904, Russia

Received: August 3, 2006; In Final Form: December 12, 2006

Multireference configuration interaction (MRD-CI) calculations are reported for a large series of electronic states of the HeNe quasimolecule up to 170000 cm^{-1} excitation energy, including those that dissociate to the $^3S_1$ and 2 $^1S_0$ excited states of the He atom. Spin−orbit coupling is included through the use of relativistic effective core potentials (RECPs). Good agreement is obtained with experimental spectroscopic data for the respective atomic levels, although there is a tendency to systematically underestimate the energies of the Ne atom by 1000−1500 cm^{-1} because of differences in the correlation effects associated with its ground and Rydberg excited states. Potential curves are calculated for each of these states, and a number of relatively deep minima are found. The CI Ω-state wave functions are sufficiently diabatic until $r = 4-5$ a_0 to allow for a clear identification of the He 1s-2s excited states. Electric dipole transition moments are computed between these states and the HeNe X 0^+ ground state up to $r = 4.0$ a_0, and it is found that the 2 $^1S_0$ - X maximum value is over an order of magnitude larger than that for the corresponding $^3S_1$ - X excitation process.

1. Introduction

The interaction of the 1s-2s excited states of the helium atom with nearly resonant metastable states of neon is known to be of great importance in inducing high-energy emission in this laser system.[1,2] In past experimental work, attention has been centered on both the He 1s-2s 2 $^1S_0$ and 1 $^3S_1$ excited states of the He atom under the influence of low-temperature collisions with Ne atoms.[3−7] It is known from atomic spectroscopy[8] that the He 2 $^1S_0$ state occurs in the same excitation energy range as Ne 2p-5s transitions, whereas the energy of the corresponding triplet state matches very closely with that of the Ne 2p-4s transitions. Potential energy curves[9] for the HeNe quasimolecule in these energy regions have been deduced earlier by employing standard semiempirical techniques, but to date no *ab initio* potentials for the same states have as yet been reported.

Probably the main reason why *ab initio* calculations are quite desirable in this type of study is that they represent the most promising means of also obtaining electric dipole transition moments for the processes of interest, which in turn are required for quantitative prediction of the intensities of these collision-induced optical transitions. Petsalakis et al.[10] made a first attempt in this direction for the HeNe system, but they only succeeded in obtaining accurate potentials and dipole moments for the relatively low-lying excited states that correlate with the 2p-3s Ne asymptotes. In the present study more extensive calculations are reported for higher-energy HeNe states that dissociate to both of the aforementioned He 1s-2s atomic limits as well as the neighboring species that correlate with the 2p-3p, 2p-4s, 2p-3d, 2p-4p, 2p-5s, and 2p-4d asymptotes, respectively.

2. Details of the Calculations

The spin−orbit interaction is essential in removing the forbidden character of the He 2s-1s transitions in the presence of neon. As in earlier work,[10] a two-step configuration interaction procedure[11,12] is employed to accomplish this task. First, Λ-S calculations are carried out at the multiconfiguration single- and double-excitation configuration interaction (MRD-CI) level of treatment with a spin-independent Hamiltonian for a large series of electronic states. The Table-Direct CI computer codes[13−15] developed in our laboratory have been employed for this purpose, but it was first necessary to construct an extended version[16] that is capable of treating as many as 30 roots of a given Λ-S symmetry in order to obtain a satisfactory description of the high-energy HeNe states of interest in the present application. The orders of the generated MRD-CI spaces vary from 760000 for the $^1A_2$ subspace to 2600000 for $^3A_1$; the corresponding secular equation sizes for the selected subspaces for which explicit diagonalizations are carried out[14] vary from 36000 to 152000. The main difficulties with the above procedure are not tied up with the rather straightforward increase in program dimensions, however, but rather in securing proper convergence for such a large number of CI roots over a broad range of internuclear distance. This objective is accomplished primarily through the inclusion of large numbers of reference configurations and by obtaining solutions for more roots of the CI secular equations than are actually required to obtain an accurate representation of the aforementioned HeNe excited states. For example, the 1s-2s He 2 $^1S_0$ state is typically the 15th root of the $^1A_1$ secular equation (in formal C_{2v} symmetry), whereas a total of 25 roots have been successfully extracted at each HeNe distance. The reason that this procedure is necessary is because the secular equation roots are not generally obtained in increasing energy order. Because of the different amounts of correlation energy for the various states, it is easily possible that their order may change significantly as the size of the CI secular equations is increased. Especially when the density of states becomes quite large as in the present case, it is therefore commonplace to first obtain a number of states in the diagonal-

* Corresponding author. E-mail: buenker@uni-wuppertal.de.
† Bergische Universitaet Wuppertal.
‡ St. Petersburg University.

10.1021/jp064987o CCC: $37.00
Published on Web 02/01/2007

ization procedure that are actually higher in energy[8] than those of lower energy that are required in a given application.

The second step in the overall procedure[11,12] is to form a contracted representation of the full spin−orbit Hamiltonian based on the above series of Λ-S states. This is another reason for obtaining more such states than the minimum number required to match the known experimental atomic states up to a given excitation energy. These calculations are carried out in the C_{2v} double group and involve basis functions of eight different symmetries ($^{3,1}A_1$, $^{3,1}A_2$, $^{3,1}B_1$, and $^{3,1}B_2$). The sizes of the corresponding secular equations are of the order of 100 in each of the four pertinent irreducible representations (Ω = A_1, A_2, B_1, and B_2). States of $\Omega = 0^+$, 2, and 4 symmetry are obtained from the A_1 secular equation, whereas those of $\Omega = 0^-$, 2, and 4 are derived from the A_2 counterpart. Odd Ω-valued states are then obtained from both the B_1 and B_2 secular equations.

The calculations are carried out with a relativistic effective core potential (RECP) for the Ne atom[17] so that only its eight valence electrons are treated explicitly in the SCF and CI calculations. The spin−orbit interaction is determined solely on the basis of the neon core potential.[11,17] The aug-cc-pVTZ basis set of Dunning[18] has been employed for the Ne atom, augmented with additional diffuse functions of s,p,d-type to describe its Rydberg excited states. A (15s9p5d2f) set of primitive gaussians is contracted to [9s7p5d2f] in these calculations. The corresponding He atomic basis is taken from Woon and Dunning.[19] It consists of a (5s4p3d) set contracted to [4s4p2d], so that a total of 95 functions are available for the SCF optimization. In constructing the He basis special attention has been paid to balancing the correlation energies of the He 1s-2s excited and $1s^2$ ground states.

The one-electron basis for the MRD-CI calculations consists of the HeNe closed-shell ground state SCF orbitals (MOs). The reference configurations have been chosen primarily to describe the set of Ne Rydberg states up to the 4d shell in the presence of the $1s^2$ He ground state configuration. In addition, the He 1s-2s $^1A_1$ and $^3A_1$ configurations are included as well, in combination with the filled shells of the Ne atomic ground state. A configuration selection threshold of $T = 0.5\ \mu$Hartree is used throughout.[14] The diagonal energies for the various Λ−S states in the spin−orbit Hamiltonian have been modified using the multireference analogue of the Davidson correction.[20,21] Finally, the MRD-CI wave functions have been employed to obtain electric dipole transition moments for the final Ω states resulting from the LSC-SO-CI treatment.[11,12]

3. Comparison with Experimental Atomic Limits

A good estimation of the overall accuracy of the present theoretical treatment for the HeNe quasimolecule can be obtained by comparing its results for the energies of the various electronic states at large internuclear separations with available experimental data for the corresponding atomic states of Ne and He.[8] Two sets of computed excitation energies are shown in Table 1, one for the HeNe system at a bond distance of $r = 30\ a_0$ and the other for the corresponding calculations carried out for the individual atoms. The latter set of results for the two atoms is obtained using the D_{2h} subgroup, thereby allowing for the solution of notably smaller CI secular equations than in the molecular calculations. Results are given for the Ne excitations from the valence 2p AO to the 3s, 3p, 4s, 3d, 4p, 5s, and 4d Rydberg orbitals, respectively.

There is a general tendency to underestimate the excitation energies within the Ne atom, but the energy order of these states is correct in all cases. The magnitude of these discrepancies is expected from analogous calculations that have been carried out for the ionization potential (IP) of the Ne atom. When the SCF−MOs of the Ne atom ground state are employed, this IP value is too low by 1565 cm^{-1}, for example. As noted above, the same choice of SCF orbitals is used for the HeNe calculations. When the SCF−MOs of the Ne+ ionic ground state are employed instead, the calculated IP value is higher by 0.05 eV (395 cm^{-1}), thereby reducing the discrepancy between theory and experiment to 1170 cm^{-1}. One also expects this IP value to be underestimated based on theoretical considerations of the respective correlation errors in the neutral and cationic systems. It is of particular importance that the amount of the energy underestimation is fairly constant throughout the entire range of Ne atom excitation energies from 130000 to 170000 cm^{-1} of interest in the present study.

The energy spacings between and within the groups of Ne 2p-3s,3p and 4s states are well described in the present SO-CI calculations. The experimental energy difference between the highest energy 3s multiplet ($J = 1°$) and the lowest of 3p type ($J = 1$) is 12369 cm^{-1}, for example, as compared to the present computed value ($r = 30\ a_0$ results, Table 1) of 12206 cm^{-1}. The difference between the highest and lowest excitation energies in the 2p-3p region of the spectrum is observed to be 4713 cm^{-1}, whereas the corresponding calculated difference is 4518 cm^{-1}. The gap between the nearest 3p and 4s energies is computed to be 5861 cm^{-1}, as compared to the corresponding observed value of 5630 cm^{-1}. The agreement is less satisfactory for the energy gap between the 4s and 3d states. The latter excitation energies are underestimated by a notably smaller margin than those discussed first. The average discrepancy between calculation and experiment is only 900 cm^{-1} for the 3d states, whereas it is 1542 cm^{-1} for the 4s states and 1561 cm^{-1} for the 4p species at somewhat higher energies. There is a similar trend for the 2p-4d states, whose excitation energies are underestimated on average by only 298 cm^{-1}.

The results for the Ne 2p-ns excitation energies are given closer consideration in Table 2. The He 1s-2s excitation energy to the triplet state (159850 cm^{-1}) lies close to those of the various 2p-4s Ne states, while that of the corresponding singlet (166272 cm^{-1}) lies between the various observed results for the corresponding 2p-5s states. The computed excitation energies for each M_J value are listed in Table 2 (using C_{2v} notation). They generally lie within 10 cm^{-1} of one another for the same J value. As already noted, the energy spacings between these states are reproduced rather well in the SO-CI calculations, with maximum discrepancies in relative energies falling in the 700 cm^{-1} range for all three groups of states.

The calculated excitation energies for the He 1s-2s singlet and triplet states are too high relative to experiment. In this case valence states are being compared, so it is not surprising that the sign of the energy discrepancies is opposite to that for the various Ne Rydberg states discussed first. The energy of the $^3S_1$ state of He is overestimated by 929 cm^{-1}, which is 0.58% of the total value. The corresponding overestimation for the 2 $^1S_0$ state is 505 cm^{-1}. This means that the triplet state lies about 2700 cm^{-1} too high in the computed spectrum than the neighboring Ne 2p-4s states. The corresponding discrepancy for the He 2 $^1S_0$ state is 1985 cm^{-1}. The influence of these computational errors on the key electric dipole transition moments for these upper states can be easily assessed by simply adjusting the He 1s-2s energy values downward by the above amounts in the second step of the LSC-SO-CI treatment in which

TABLE 1: Comparison of Observed[8] and Calculated Ne Atom Excitation Energies (cm^{-1})

upper AO	J	exptl	$r = 30\ a_0$	calcd − obsd	Ne atom	calcd − obsd	Δ calcd
3s	2°	134044	132975	−1069	132886	−1158	−89
	1°	134461	133205	−1256	133116	−1345	−89
	0°	134821	133355	−1466	133265	−1556	−90
	1°	135891	134620	−1271	134575	−1316	−45
3p	1	148260	146826	−1434	146708	−1552	-118
	3	149659	148402	−1257	148335	−1324	−67
	2	149826	148523	−1303	148462	−1364	−61
	1	150124	148680	−1444	148653	−1471	−27
	2	150318	148986	−1332	148947	−1371	−39
	0	150919	149303	−1616	149264	−1655	−39
	1	150774	149301	−1473	149244	−1530	−57
	2	150860	149310	−1550	149306	−1554	−4
	1	151040	149465	−1575	149432	−1608	−33
	0	152973	151344	−1629	151272	−1701	−72
4s	2°	158603	157205	−1398	157202	−1401	−3
	1°	158797	157347	−1450	157365	−1432	18
	0°	159382	157586	−1796	157588	−1794	2
	1°	159537	157746	−1791	157803	−1734	57
He 1s-2s triplet	1	159850	160779	929			
3d	0°	161512	160839	−673	160846	−666	7
	1°	161526	160841	−685	160849	−677	8
	4°	161592	160856	−736	160887	−705	31
	3°	161594	160880	−714	160890	−704	10
	2°	161609	160887	−722	160896	−713	9
	1°	161639	160908	−731	160901	−738	−7
	2°	161702	160920	−782	160943	−759	23
	3°	161703	160943	−760	160946	−757	3
	2°	162411	161003	−1408	161287	−1124	284
	3°	162412	161260	−1152	161290	−1122	30
	2°	162421	161285	−1136	161296	−1125	11
	1°	162438	161294	−1144	161297	−1141	3
4p	1	162520	161300	−1220	160977	−1543	−323
	3	162833	161385	−1448	161382	−1451	−3
	2	162901	161445	−1456	161442	−1459	−3
	1	163015	161546	−1469	161560	−1455	14
	2	163040	161585	−1455	161594	−1446	9
	0	163403	161812	−1591	161820	−1583	8
	1	163659	161833	−1826	161817	−1842	−16
	2	163711	161868	−1843	161890	−1820	23
	1	163710	161906	−1804	161908	−1802	2
	0	164288	162532	−1756	162524	−1764	−8
5s	2°	165830	164694	−1136	164731	−1099	37
	1°	165915	164769	−1146	164883	−1032	114
He 1s-2s singlet	0	166272	166777	505			
	0°	166608	165075	−1533	165154	−1454	79
	1°	166658	165126	−1532	165241	−1417	115
4d	0°	166970	166272	−698	165904	−1066	−368
	1°	166977	166272	−705	165905	−1072	−367
	4°	167002	166530	−472	165918	−1084	−612
	3°	167003	166628	−375	165920	−1083	−708
	2°	167013	166693	−320	165923	−1090	−770
	1°	167029	166960	−69	165928	−1101	−1032
	2°	167050	166996	−54	165939	−1111	−1057
	3°	167050	167208	158	165942	−1108	−1266
	2°	167797	167407	−390	166305	−1492	−1102
	3°	167798	167436	−362	166306	−1492	−1130
	2°	167799	167457	−342	166309	−1490	−1148
	1°	167810	167460	−350	166310	−1500	−1150

the full spin−orbit Hamiltonian is diagonalized in the contracted Λ−S basis, as will be discussed in Section V.

4. Computed Potential Energy Curves

The spin−orbit CI calculations described in Section 2 produce the set of Ω-state HeNe potential curves shown in Figure 1a. The various Ne-state asymptotic energy values at $r = 30\ a_0$ are the same as in Table 1. There is relatively little change in these values until an internuclear separation of $r = 8\ a_0$ is reached. The potential curves that dissociate to the Ne 2p-3d limit have been omitted in this diagram in order to make it easier to identify their He 1s-2s counterparts. As noted in Table 1, these Ne 3d states occur in a fairly narrow range of energy (160800−161300 cm^{-1} in the calculations). Their potential curves over a relatively small range of internuclear distance will be considered subsequently.

In Figure 1a the key He $^3S_1$ potential curves are found to lie just below those of the Ne 4p states. As already mentioned in Section 2, there is a systematic underestimation of the energies of the Ne states in the present theoretical treatment because of the greater correlation energy of the corresponding ground state. At the same time, the energies of the He 1s-2s states are overestimated by 500−900 cm^{-1}. To investigate the effects of these errors on the spin−orbit CI treatment, additional calcula-

TABLE 2: Computed Excitation Energies (cm^{-1}) for Different Ω-Components (C_{2v} Double Group Notation) of the Ne 2p-ns States Treated in the Present Study

		A_1	A_2	B_1	B_2	average
$n=3$	$J=2°$	132984	132966	132970	132970	132975
			132984			
	$J=1°$	133213		133201	133202	133205
	$J=0°$		133355			133355
	$J=1°$	134605		134628	134628	134620
$n=4$	$J=2°$	157210	157200	157202	157203	157205
			157210			
	$J=1°$	157346		157348	157348	157347
	$J=0°$		157586			157586
	$J=1°$	157736		157751	157752	157746
$n=5$	$J=2°$	164700	164688	164691	164690	164694
			164700			
	$J=1°$	164764		164771	164771	164769
	$J=0°$		165075			165075
	$J=1°$	165122		165128	165128	165126

tions have been carried out by shifting the potentials of the He 1s-2s states downward so that they have nearly the same relation to the neighboring Ne potentials as is known from experimental atomic data.[8] This was done by altering the diagonal energies in the SO-CI Hamiltonian matrix by −2715 and −1985 cm^{-1}, respectively, for the He 1s-2s triplet and singlet excited states. The resulting Ω-state potential curves are shown in Figure 1b for comparison with the corresponding unshifted results. The shapes of the various potential curves are not changed significantly by this procedure, as is expected based on the rather small magnitudes of the various spin−orbit matrix elements for this relatively light system. At small internuclear distances ($r < 4.0$ a0), it becomes progressively more difficult to assign the potentials to a particular diabatic configuration because of the increased mixing between the Ne and He excited states. We will return to this point when the He 1s-2s potentials and transition moments are discussed below.

The individual groups of the excited HeNe quasimolecular states are considered next, starting with the Ne 2p-3s species. Their spin−orbit potential curves are shown in Figure 2 (the energies of the Ne states have been shifted upward by 1000 cm^{-1} in all the following diagrams so as to have better agreement with the corresponding experimental values, but those of the He states have been left unshifted). As already noted in Table 1, the order and energy separations of these states at large r values is in good agreement with the known experimental asymptotic results for the Ne atom. The lowest-energy such state has $J = 2°$ symmetry. The corresponding Ω-state potential curves lie very close to one another until the HeNe distance reaches approximately 5.0 a_0, in which region the $\Omega = 2$ curve becomes notably more repulsive than the other two components of $\Omega = 1$ and 0^- symmetry. The latter two states remain nearly degenerate at all distances considered and reach a maximum in energy near $r = 4.0$ a_0. A potential minimum occurs near $r = 3.0$ a_0 before the curves become repulsive at shorter separations. None of these states is bound relative to their dissociative atoms, however. A similar pattern is found for the next set of curves that dissociate to the $J = 1°$ atomic state of Ne (Figure 2). In this case, it is the $\Omega = 0^+$ state that possesses an inner minimum in its potential, whereas the corresponding $\Omega = 1$ curve is purely repulsive. The next-highest HeNe state dissociates to the nondegenerate $J = 0°$ Ne state. It has $\Omega = 0^-$ symmetry and possesses a purely repulsive potential curve. There is a fairly large energy gap between this state and the last member ($J = 1°$) of the Ne 3s group of atomic limits. The corresponding potentials are both repulsive, although the $\Omega=0^+$ curve is notably less steep.

The calculated spin−orbit CI potential curves for the Ne 2p-4s and He 1s-2s $^3S_1$ electronic states are shown in Figure 3. The latter state is found experimentally to lie only 313 cm^{-1} above the highest-lying ($J = 1°$) Ne 2p-4s state, whereas the computed energy difference is about 1900 cm^{-1} in the diagram. The Ne 4s asymptotic states are in the same energetic order as for their 3s counterparts shown in Figure 2. Again, the potentials of the Ω-components of the $J = 2°$ atomic state are seen to diverge from one another as the internuclear distance is decreased. The $\Omega = 1$ and 0^- potentials nearly coincide for the entire range of distances considered and approach their respective minima at $r < 3.5$ a_0. The corresponding $\Omega = 2$ curve shows a maximum near $r = 4.0$ a_0, unlike the case for the Ne 2p-3s states. The potentials for the next-highest atomic limit ($J = 1°$) also start to diverge for $r < 5.4$ a_0, with the $\Omega = 0^+$ state having a minimum in the same range as the $\Omega = 1$ and 0^- states already discussed. None of the 2p-4s states is repulsive according to the present calculations, in contrast to those of 2p-3s type. A number of them exhibit shallow minima in the $r = 4-5$ a_0 region before reaching a maximum near $r = 4.0$ a_0.

The He 1s-2s $^3S_1$ potential has an absolute minimum at $r = 4.50$ a_0. The depth of the potential well is 487 cm^{-1}. There are two nearly degenerate components ($\Omega = 1$ and 0^-), consistent with the relatively small spin−orbit effects expected for such a light atom. The computed spin−orbit CI energies for both the singlet and triplet He 1s-2s excited states as well as the ground state are given in Table 3 for the range of internuclear separation between 3.0 and 30.0 a_0. The He $^3S_1$ state also possesses a potential minimum at larger distance ($r = 9-10$ a_0). The well depth in this case is only 78 cm^{-1}, however. This minimum corresponds to that found experimentally by Patil et al.[22] at $r = 10.4$ a_0, with a well depth of only 5.64 cm^{-1}. The overestimation of the well depth at such large r values is quite consistent with the error limits expected for this level of treatment (0.01−0.02 eV or 80−160 cm^{-1}). A potential maximum is found near $r = 7.0$ a_0, at which point the energy of this state is computed to be 6 cm^{-1} higher than for the separated atoms. Beyond $r = 4.0$ a_0, the $^3S_1$ potential curve becomes repulsive, increasing by 5700 cm^{-1} above its minimal energy value at $r = 3.0$ a_0. The He $^1S_0$ ground state potential has notably less binding energy, reaching a minimum energy value of 24 cm^{-1} near $r = 6.0$ a_0. Keil et al.[23] have reported a potential minimum for this state at $r = 5.72$ a_0, with a well depth of 14.8 cm^{-1}.

The spin−orbit CI potential curves for the Ne 2p-5s and He 1s-2s $^1S_0$ states are shown in Figure 4 (as mentioned above, the former states are shifted upward in this diagram by 1000 cm^{-1}). As shown in Table 1, the corresponding asymptotic energy is only 336 cm^{-1} higher in the experimental spectrum than that of the Ne 2p-5s 0° state. The He $^1S_0$ potential has a shallow minimum near $r = 11.0$ a_0 (see Table 3) with a well depth of 126 cm^{-1}. The latter result greatly overestimates the experimental value of only 3.31 cm^{-1} reported by Patil et al. .[22] The calculations indicate that a potential maximum is reached in the $r = 6-7$ a_0 range before an absolute minimum in energy is found at $r = 5.0$ a_0. The corresponding well depth is computed to be 220 cm^{-1} in this case. In general, the results for the absolute potential minima for the He 1s-2s^{3,1}S states of He obtained in the present study confirm the qualitative discussion given in ref 9. The potential curve becomes quite repulsive after this point. As before with the He $^3S_1$ calculated well depths, it needs to be emphasized that the error limits for the present calculations are expected to be in the order of a few hundredths of an eV, as demonstrated by the scatter in the individual energy

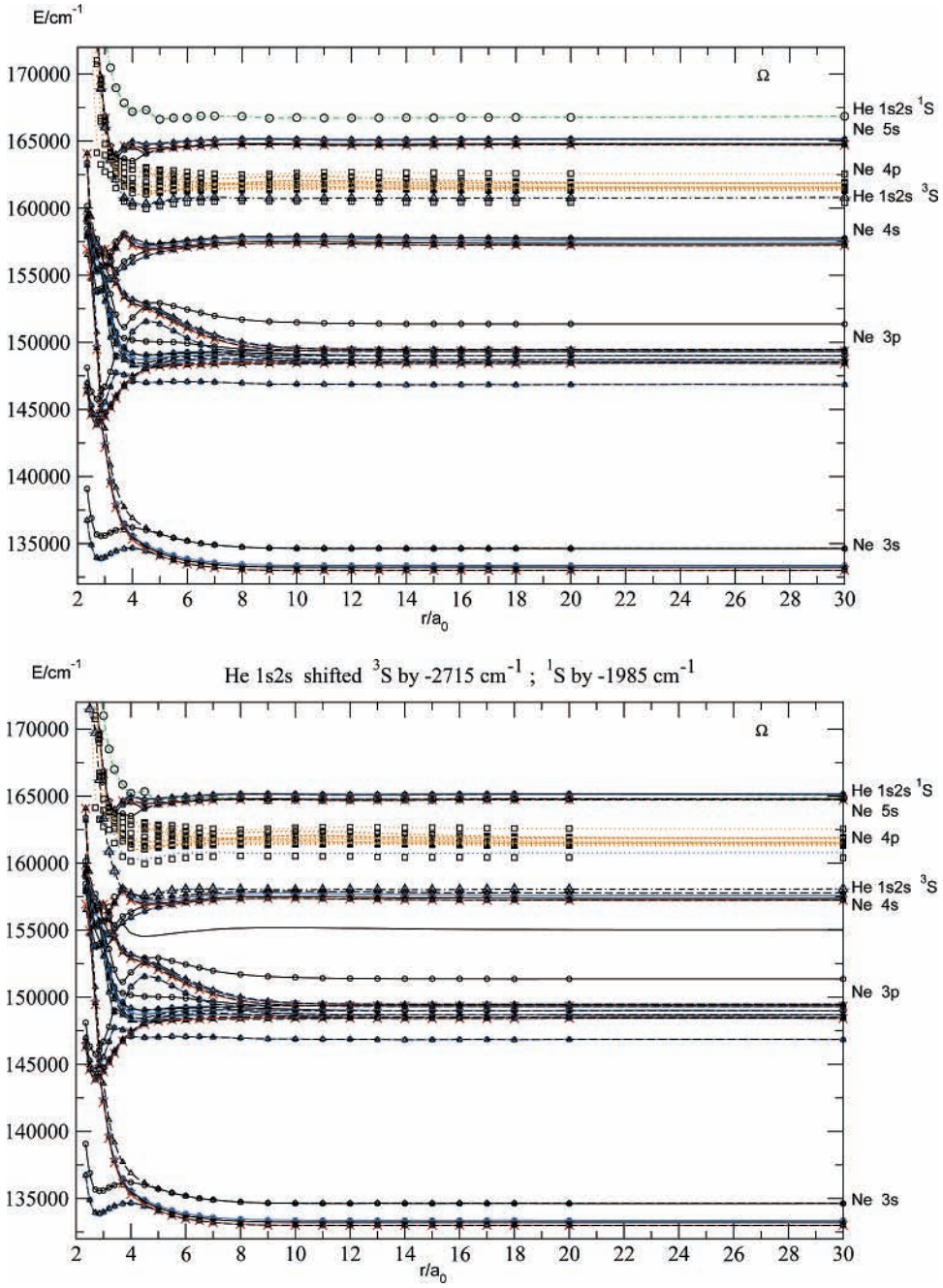

Figure 1. Calculated MRD-SO-CI potential energy curves for various excited states of the HeNe quasimolecule (energy in cm^{-1}, bond distance in a_0) in the 135000−170000 cm^{-1} range: (a) directly computed and (b) obtained by empirically shifting the diagonal energies of the He excited states in the spin−orbit Hamiltonian matrix by the amounts shown.

points themselves vis-à-vis the fitted potential data in Figure 4. The composition of the associated wave functions is nonetheless expected to be of quite suitable accuracy for the prediction of electronic transition moments, which are much more difficult to measure experimentally.

The neighboring Ne 2p-5s states have similarly shaped potentials as their 4s counterparts shown in Figure 3 down to a He−Ne separation of about $r = 5.0$ a_0. The lowest energy for this group of states occurs near $r = 4.0$ a_0 for the 0^+ component of the $J = 1°$ asymptote. All of the other states of this group have a potential maximum in this region. They each have rather significant minima at around $r = 3.4$ a_0, at which point the energies of the latter 0^+ state and the $1,0^-$ components of the $J = 2°$ asymptote become very nearly equal. The spin−orbit energy splittings between the various *J*-component asymptotic limits is reproduced rather well in the calculations (see Table 1), especially considering that they are high-lying roots in the spin−orbit CI secular equations. The 2° and lower 1° states are separated by only 75 cm^{-1} in the calculations, as compared to the experimental splitting of 85 cm^{-1}, for example. The corresponding gap between the upper 1° state and 0° is computed to be 51 cm^{-1}, only 1 cm^{-1} less than the corresponding measured value. The gap between these two pairs of states is underestimated in the present spin−orbit CI treatment (306 cm^{-1} vs 693 cm^{-1}), however.

The potential curves that correlate with the Ne 2p-3p limit are shown in Figures 5a−c. Transitions from these states to the Ne ground state are forbidden by the parity selection rule. In order to better distinguish between individual potentials, the curves have been divided up according to their Ω values in the C_{2v} double group in which the HeNe calculations are actually carried out in the present study. It should be noted that the $J =$

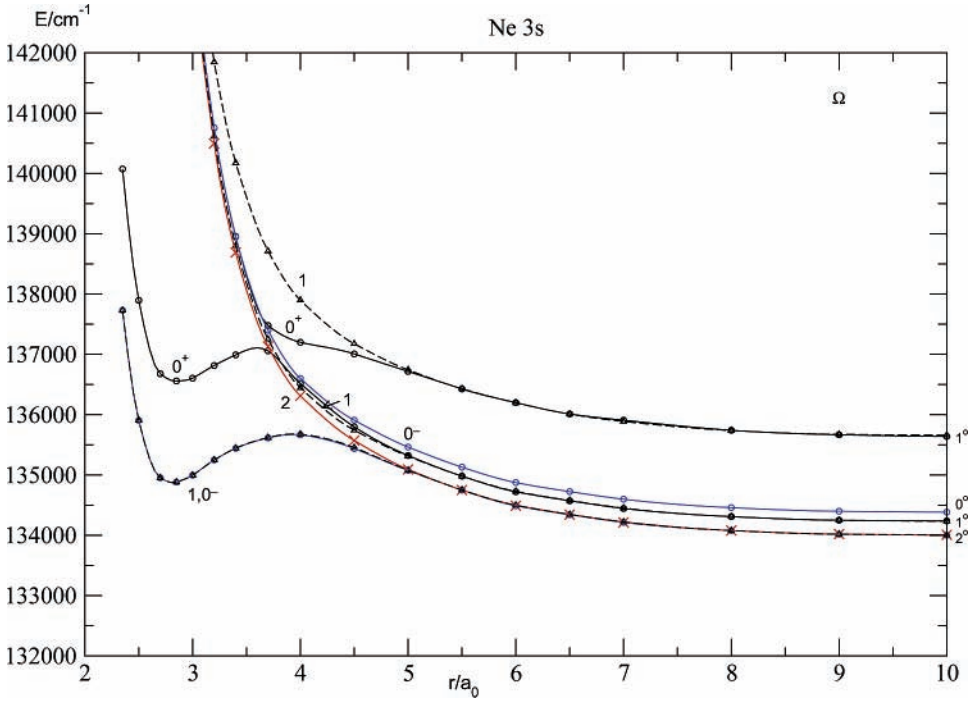

Figure 2. Computed MRD-SO-CI potential energy curves for the electronic Ω-states of the HeNe quasimolecule that correlate with the Ne 2p-3s atomic limits (energy in cm^{-1}, bond distance in a_0).

TABLE 3: Calculated Spin−Orbit CI HeNe Potential Energies (cm^{-1}) for Ω-States (Linear Double Group Notation) That Correlate with the Atomic Limits of the He Atom (Internuclear Distance *r* in a_0).

r	X 0^+	0^- (He $^3S_1$)	1 (He $^3S_1$)	0^+ (He 2 $^1S_0$)
3.00	6674	166060	166058	172977
3.20	4142	163596	163591	170486
3.40	2542	162133	162134	168979
3.70	1209	160758	160764	167854
4.00	562	160399	160378	167196
4.50	144	160316	160315	167324
5.00	31	160490	160490	166631
5.50	8	160665	160666	166731
6.00	0	160768	160769	166724
6.50	13	160789	160789	166872
7.00	18	160809	160809	166878
8.00	19	160762	160762	166847
9.00	20	160733	160733	166707
10.00	22	160725	160725	166752
11.00	18	160746	160746	166725
12.00	20	160761	160761	166730
13.00	23	160749	160749	166738
14.00	21	160749	160749	166747
15.00	23	160738	160738	166739
16.00	23	160751	160751	166765
17.00	23	160760	160760	166765
18.00	21	160778	160778	166769
20.00	20	160770	160770	166765
30.00	24	160803	160803	166851

0 and 3 states each have one A_1 Ω component (0^+ and 2, respectively), whereas $J = 2$ has two such components (0^+ and 2) and $J = 1$ has none. These potentials are shown in Figure 5a. The corresponding potential curves in the A_2 subspace include the 0^- components of the $J = 1$ and 3 multiplets, one of which is the lowest in the Ne 2p-3p portion of its spectrum (see Table 1). The $J = 2$ multiplets have one A_2 component, each of which is degenerate with the corresponding $\Omega = 2$ state in the A_1 subspace. There are three such states and their associated potential curves are easily identified on this basis in Figures 5a,b. The lowest of these exhibits an attractive branch to its potential in the $r = 3-5$ a_0 region, for example. The other potential curve correlating with this $J = 2$ atomic limit belongs to the $\Omega = 0^+$ manifold of states, which therefore only appears in Figure 5a. It has a minimum near $r = 4.5$ a_0, followed by a distinct maximum near $r = 3.5$ a_0. There is also a $\Omega = 2$ degenerate pair for the $J = 3$ atomic limit in the A_1 and A_2 subspaces (the lowest curve in Figure 5a). Finally, the $\Omega = B_1$ potential curves in Figure 5c correspond to $\Omega = 1$ and 3 in the linear double group. The $J = 3$ atomic limit correlates with one state of each of the above symmetries, all others with only one, namely that with $\Omega = 1$. The lowest three states in this subspace have rather deep potential wells whose minima occur for $r < 3$ a_0 and thus are not shown in Figure 5c. The rather large spin−orbit splitting between the $J = 1$ and 3 atomic limits is computed to have a value of 1576 cm^{-1} (Table 1), which compares reasonably well with the experimental result of 1399 cm^{-1}. The existence of absolute minima for some of the states produced by the $He^{3,1}S$ and Ne 4s, 5s and 3p states are similar to those obtained in the framework of the effective Hamiltonian method[24,25] for distances in the 8−12 a_0 range.

The Ne 2p-3d states lie just above the 2p-4s species and the He $^3S_1$ state already discussed (see Table 1). Their potential curves are shown in Figures 6a−c but are not included in the composite potential diagrams of Figures 1a,b. The states are again divided into C_{2v} double group sets. The lowest-energy of these states at small *r* values has $\Omega = 0^+$ symmetry and correlates with the 1° atomic limit, which is second-lowest J-state asymptote among the Ne 2p-3d states. As such, it appears in the $\Omega = A_1$ subspace but not in A_2. It has a binding energy in excess of 2500 cm^{-1} according to the spin−orbit CI calculations. The states divide into two subsets in the $r = 8-10$ a_0 region. Almost all the corresponding potentials in the lower-energy set have an attractive portion between $r = 4$ and 6 a_0. For $r > 10$ a_0 several of the curves in the upper group turn downward so that at $r = 15$ a_0, only the Ω states associated with the highest three 2p-3d atomic limits ($J = 3° < 2° < 1°$, see Table 1) remain above this energy gap. Even the higher states possess a small well in their potentials, usually in the neighborhood of $r = 4$ a_0.

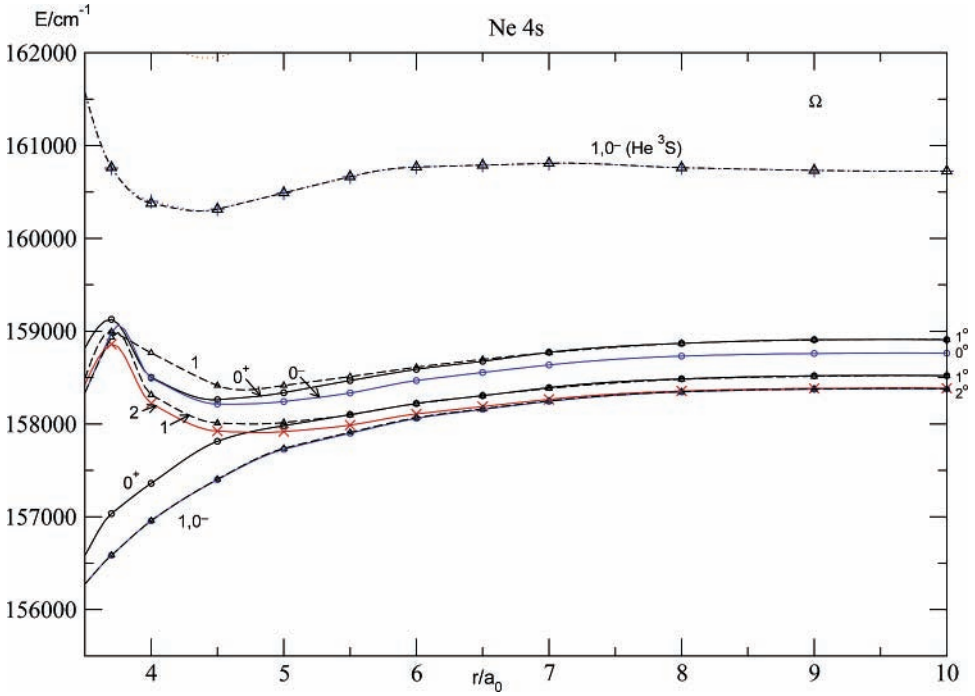

Figure 3. Computed MRD-SO-CI potential energy curves for the electronic Ω-states of the HeNe quasimolecule that correlate with the Ne 2p-4s and He 1s-2s $^3S_1$ atomic limits (energy in cm^{-1}, bond distance in a_0).

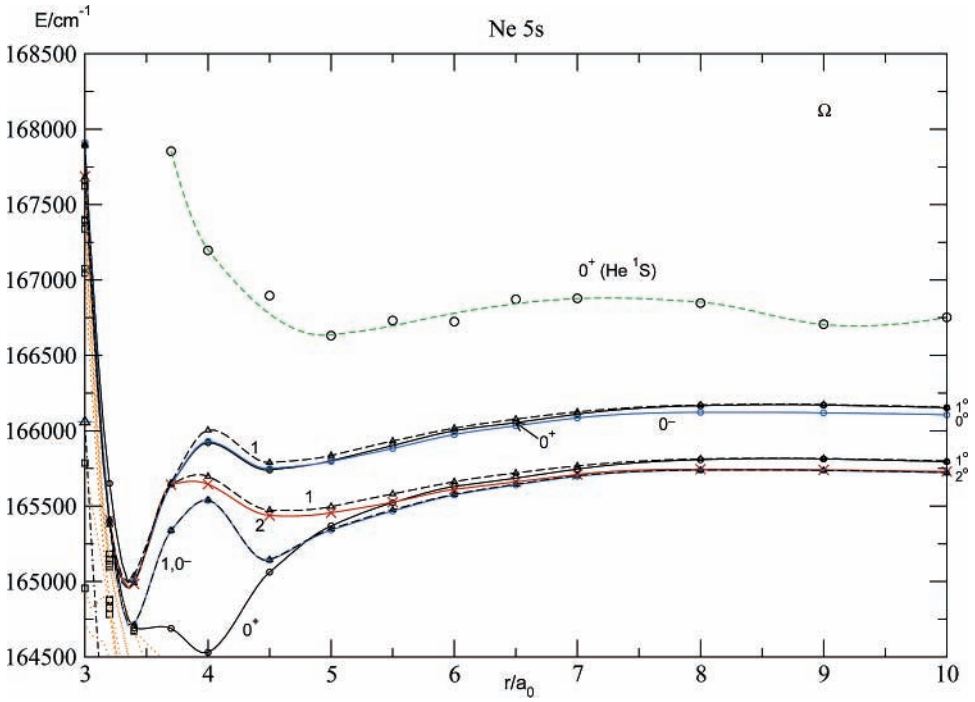

Figure 4. Computed MRD-SO-CI potential energy curves for the electronic Ω-states of the HeNe quasimolecule that correlate with the Ne 2p-5s and He 1s-2s $^1S_0$ atomic limits (energy in cm^{-1}, bond distance in a_0).

The Ne 2p-4p states lie between the 2p-3d and 2p-5s states (Table 1) and their computed NeHe potential curves are shown in Figures 7a−c. The corresponding asymptotes are found in a range of about 2000 cm^{-1}, with a gap of more than 1500 cm^{-1} separating them from the lowest 2p-5s levels (see Figure 1a). In the case of the $\Omega = A_2$ and B_1 states, it has proven quite difficult to identify them for $r < 4.5$ a_0, and hence the potentials for these states are only shown up to that distance. The lowest two states have dissociation energies of about 500 cm^{-1} (Figure 7a), corresponding to symmetries of 0^+ and 2, respectively.

5. Electric-Dipole Transition Moments

The spin−orbit CI wave functions have been employed to calculate electric dipole transition moments between each of the HeNe Ω-states at all internuclear distances considered above. Only transitions to the HeNe X $^1S_0$ ground state will be discussed in the following. The 2p-ns 1°-X are the strongest transitions in the Ne atomic spectrum. There are two such upper states for each value of n, corresponding to the triplet and singlet Λ−S states, respectively. At $r = 30$ a_0 for the 3s states, values of 0.0465 and 0.3512 ea_0, respectively, are obtained. Since the

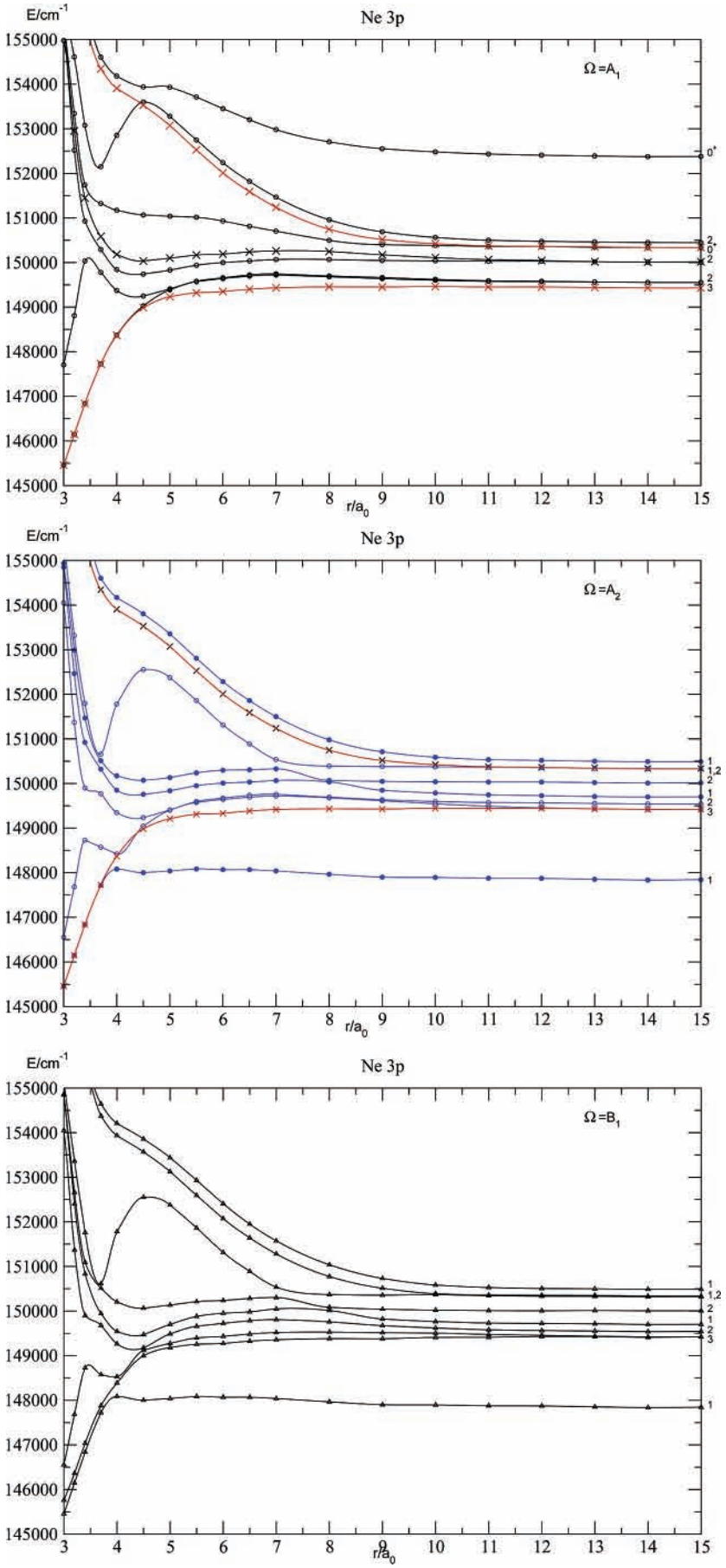

Figure 5. Calculated MRD-SO-CI potential energy curves for the electronic Ω-states of the HeNe quasimolecule that correlate with the Ne 2p-3p atomic limits (energy in cm^{-1}, bond distance in a_0) belonging to the Ω = (a) A_1, (b) A_2, and (c) B_1 irreducible representations of the C_{2v} double group.

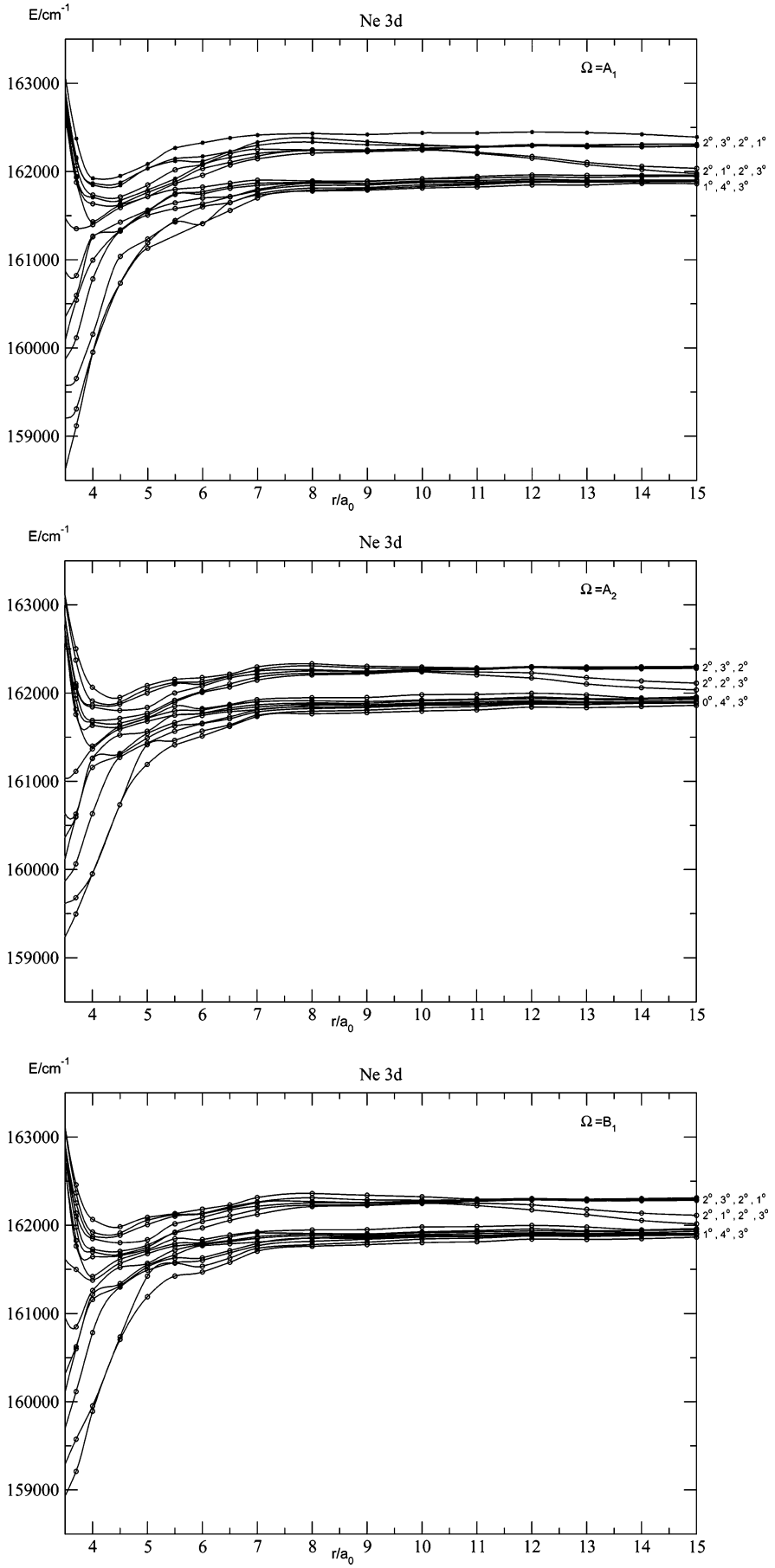

Figure 6. Calculated MRD-SO-CI potential energy curves for the electronic Ω-states of the HeNe quasimolecule that correlate with the Ne 2p-3d atomic limits (energy in cm^{-1}, bond distance in a_0) belonging to the Ω = (a) A_1, (b) A_2, and (c) B_1 irreducible representations of the C_{2v} double group.

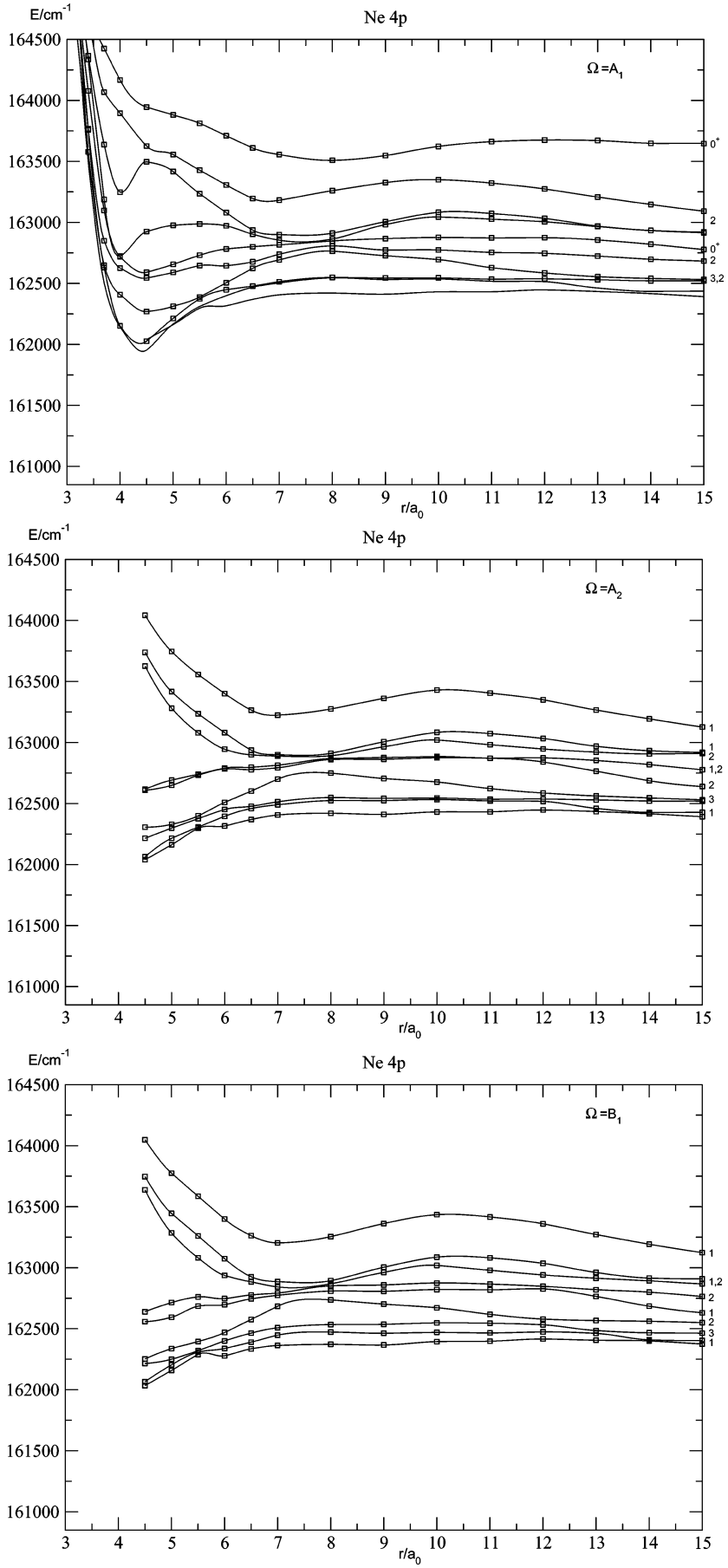

Figure 7. Calculated MRD-SO-CI potential energy curves for the electronic Ω-states of the HeNe quasimolecule that correlate with the Ne 2p-4p atomic limits (energy in cm^{-1}, bond distance in a_0) belonging to the Ω = (a) A_1, (b) A_2, and (c) B_1 irreducible representations of the C_{2v} double group.

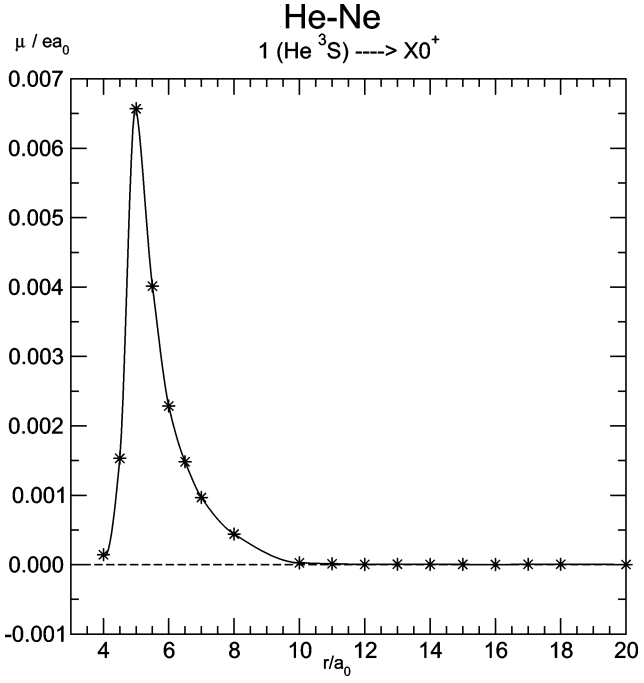

Figure 8. Computed MRD-SO-CI electronic dipole transition moment μ (ea_0) between the electronic Ω-states that correlate with the X 0^+ ground state and the $1\ ^3S_1$ excited-state of the He atom as a function of the HeNe internuclear distance r (a_0).

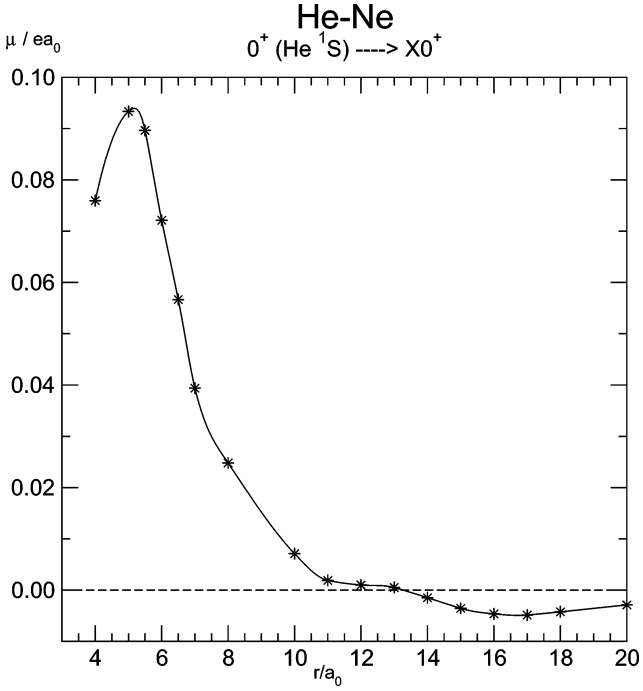

Figure 9. Computed MRD-SO-CI electronic dipole transition moment μ (ea_0) between the electronic Ω-states that correlate with the X 0^+ ground state and the $2\ ^1S_0$ excited-state of the He atom as a function of the HeNe internuclear distance r (a_0).

former transition is spin-forbidden, these results are a good indication of the role that spin−orbit coupling plays in determining the wave functions for this rather light system. The corresponding values for the 2p-4s 1° states are 0.0761 and 0.1151 ea^0. The fact that the latter two results are closer together in magnitude is a manifestation of the fact that the energy difference between the two states is considerably smaller than for their 3s counterparts, which is expected based on the greater diffuseness of the 4s orbital. This characteristic also explains why the average magnitude is notably larger for the 2p-3s states. For $n = 5$ both trends continue. The two values are nearly equal (0.0669 and 0.0620 ea_0), and the higher-energy value is actually somewhat smaller in this case.

The values of the Ne 2p-ns transition moments remain very nearly constant as the He atom approaches until a distance of about $r = 6-7$ a_0 is reached. The value of the He $^3S_1-X$ transition moment is very close to zero until the Ne atom comes into the same range. The computed variation of this transition moment with r is shown in Figure 8. The dipole moment for the He ^3S state in the presence of a Ne atom has been calculated for the first time in the present work. The corresponding atomic transition is forbidden by both spatial and spin selection rules, so the latter result is hardly surprising. The fact that both atoms are relatively light means that the effects of spin−orbit coupling are never very strong in this system, however, so the increase in the value of this transition moment at shorter r values is moderate at best. The present calculations indicate that a maximum is reached near $r = 5$ a_0, with a value of only 0.0066 ea_0 (see Table 4). Another indication of the weakness of the spin−orbit effects is the fact that the energies of the respective $= 1$ and 0^- components of the He $^3S_1$ state are very close to the same for the entire HeNe distance range considered (Figure 4). The transition moment shown in Figure 8 is for the $\Omega = 1$ component, whereby the corresponding value for the 0^--X component is zero by symmetry. Especially since the value of the 1-X transition moment decreases to nearly zero at $r = 4.0$ a_0, it seems clear that it will be very difficult to observe this process by conventional spectroscopic techniques. It also should be recalled that the upper state in question lies only slightly above the higher 1° member of the 2p-4s group of states (Figure 3 and Table 1), so such a weak transition would have to be detected in the relatively strong background associated with these other upper states.

TABLE 4: Calculated Electric Dipole Transition Moments (ea_0) from the He 1s-2s Excited States to the X 0^+ Ground State of the HeNe Quasimolecule as a Function of Internuclear Distance r (a_0)

r	He 1 ($^3S_1$) - X 0^+	He 0^+ ($2\ ^1S_0$) - X0^+
4.00	0.000143	0.075945
5.00	0.006569	0.093345
5.50	0.004013	0.089641
6.00	0.002286	0.072119
6.50	0.001482	0.056647
7.00	0.000968	0.039380
8.00	0.000441	0.024791
10.00	0.000026	0.007111
11.00	0.000013	0.001889
12.00	0.000003	0.000986
13.00	0.000006	0.000508
14.00	0.000003	0.001486
15.00	0.000003	0.003554
16.00	0.000002	0.004629
17.00	0.000005	0.004856
18.00	0.000006	0.004236
20.00	0.000002	0.002899
30.00	0.000000	0.002927

The possibilities of detecting emission out of the He 1s-2s singlet state in Ne atom collisions is far greater, however. Previous calculations for this process have been carried out by employing the effective Hamiltonian method for distances between 8 and 12 a_0.[26,27] The corresponding transition moment curve calculated for this process in the present work is shown in Figure 9. It also has maximum near $r = 5$ a_0, but its value at that point is 0.0933 ea_0 and thus is much greater than for the $^3S_1-X$ transition (Table 4). Since the oscillator strength is proportional to the square of the transition moment, this means

that HeNe ground state transitions from the He 1s-2s singlet state should be over 2 orders of magnitude stronger than for the corresponding triplet state. Examination of the relevant wave functions shows that spin−orbit coupling has very little influence on the latter result. Instead, it is found that both the He 1s and 2s orbitals take on considerable Ne 2pσ character as the distance to the Ne atom is decreased. In effect, what one has at small r values are spin-allowed transitions between He s and Ne p AOs. It becomes difficult to assign a particular Ω-state as the one with diabatic He 1s-2s $^1S_0$ character beyond $r = 4$ a_0 because the HeNe MOs take on such mixed character in this region. Hence, transition moment results are only given in Table 4 up to this HeNe distance. If one sums up the oscillator strengths from all neighboring transitions whose upper state has at least partial He 2 $^1S_0$ character, the indication is that the intensity of He 1s-2s transitions to the HeNe ground state continues to increase for $r < 5$ a_0.

6. Conclusion

In attempting to describe atomic and molecular collision processes with ab initio quantum mechanical calculations, one is confronted with the fact that the density of states is often significantly increased beyond that which exists for an isolated collision partner. The present study has dealt with a classic example of this type, namely the interaction of the 1s-2s excited states of the helium atom with the large number of Rydberg states of the Ne atom in the same energy range. In order to obtain a reliable description of the associated HeNe quasimolecular states over a wide range of internuclear distance, it is necessary to obtain as many 30 roots of a given CI secular equation. A good rule is to obtain results for at least several roots of higher energy than those of immediate interest in a given problem. The problem is exacerbated when spin−orbit coupling plays a significant role in the theoretical treatment, since its inclusion leads to the removal of degeneracies that are present in conventional spin-independent (Λ-S) calculations. In order to describe the He 1s-2s $^1S_0$ excited-state in the presence of a single neon atom, for example, this means that results must be obtained for the 49th root of the relevant secular equation.

The present multireference spin−orbit CI treatment leads to an underestimation of the Ne atom excitation energies by 1000−1500 cm^{-1} because of the smaller amount of correlation energy associated with the Rydberg states of this system vis-à-vis that of its closed-shell ground state. At the same time, the 1s-2s excitation energies of He have been overestimated by 505 and 929 cm^{-1}, respectively. Tests have been made by shifting the diagonal (Λ-S) energies in the spin−orbit Hamiltonian matrix to obtain improved agreement with the experimental asymptotic energies for the HeNe system, and they have indicated that neither the shapes of the molecular potential curves nor the values of properties such as dipole transition moments are significantly affected by such a procedure. In particular, it has been possible to easily distinguish the key He 1s-2s excited states from their Ne Rydberg counterparts up to internuclear distances as small as $r = 4$ a_0. It seems clear that this simplifying feature of the molecular calculations is due primarily to the weakness of the spin−orbit interaction for such light elements, and thus that it will prove to be more of an exception rather than the rule in analogous treatments for heavier atoms.

The calculations indicate that both the He 1s-2s states have short-range potential minima near $r = 5$ a_0, with that of the triplet state being notably deeper (ca. 500 cm^{-1}). Comparison with experimental data for known minima at larger r values indicates that the present treatment tends to overestimate such quantities by on the order of 100 cm^{-1}, however. The area in which the present calculations are expected to be most valuable is in the prediction of dipole transition moments, which are quite difficult to derive from experimental data alone. It is found that the $^3S_1-X$ transition moment remains small at all internuclear distances, reaching a value of 0.0066 ea_0 for $r = 5.00$ a_0. This result again shows that there is relatively little spin−orbit mixing in this light system to overcome the spin-forbiddenness of such transitions for the isolated He atom. The corresponding maximal value for the $^1S_0-X$ transition moment is nearly 15 times larger, also in the neighborhood of $r = 5.00$ a_0. Examination of the relevant wave functions for these states shows that the main reason for the relatively large increase in this quantity is the admixture of Ne 2pσ character in both the He 1s and 2s orbitals at small r values.

Acknowledgment. The authors (A.D. and R.B.) are grateful for the support of the Deutsche Forschungsgemeinschaft under grant BU 450/17-1. One of us (A.D) is grateful for the hospitality shown him by the University of Wuppertal during his recent visit.

References and Notes

(1) Shalabi, A. S.; Assem, M. M.; Abd El-Aal, S.; Kamel, M. A.; Abd El-Rahman, M. M. *Eur. Phys. J. D:* **1999**, *7*, 181.
(2) Devdariani, A. Z.; Chesnakov, E. A. *Opt. Spectrosc.* **2005**, *99*, 866.
(3) Haberland, H.; Konz, W.; Oeslerlin, P. *J. Phys. B: At. Mol. Phys.* **1982**, *15*, 2969.
(4) Haberland, H.; Oeslerlin, P. *Z. Phys. A* **1982**, *304*, 11.
(5) Chen, C. H.; Haberland, H.; Lee, Y. T. *J. Chem. Phys.* **1974**, *61*, 3095.
(6) Fukuyama, T.; Siska, P. E. *Abstracts of the 11th International Conference on the Physics of Electronic and Atomic Collisions*; The Society for Atomic Collisions Research: Kyoto, 1979; p 460.
(7) Fukuyama, T.; Siska, P. E. *Abstracts of the 10 International Conference on the Physics of Electronic and Atomic Collisions*; Commissariat a l' Energie Atomique: Paris, 1977; p 552.
(8) Moore, C. E. *Atomic Energy Levels as Derived from the Analyses of Optical Spectra*; Circular of the National Bureau of Standards 467, National Bureau of Standards: Gaithersburg, MD, 1949; Vol. 1.
(9) Devdariani, A. Z.; Buenker, R. J. *Khim. Fys.* **2004**, *23* (2), 61.
(10) Petsalakis, I. D.; Theodorakopoulos, G.; Liebermann, H.-P.; Buenker, R. J. *J. Chem. Phys.* **2001**, *115*, 6365.
(11) Buenker, R. J.; Alekseyev, A. B.; Liebermann, H.-P.; Lingott, R.; Hirsch, G. *J. Chem. Phys.* **1998**, *108*, 3400.
(12) Alekseyev, A. B.; Liebermann, H.-P.; Buenker, R. J. In *Relativistic Molecular Calculations*; Hirao, K., Ishikawa, M., Eds.; World Scientific: Singapore, 2003; p 65.
(13) Buenker, R. J.; Krebs, S. In *Recent Advances in Multireference Methods*; Hirao, K., Ed.; World Scientific: Singapore, 1999; p 1.
(14) Krebs, S.; Buenker, R. J. *J. Chem. Phys.* **1995**, *103*, 5613.
(15) Buenker, R. J. In *Proceedings of the Workshop on Quantum Chemistry and Molecular Physics*; Burton, P. G., Ed.; University of Wollongong Press: Wollongong/Australia, 1980, p 1.5.1. Buenker, R. J. In *Current Aspects of Quantum Chemistry*; Carbo, R., Ed.; Elsevier: Amsterdam, 1982; Vol. 21, p 17. Buenker, R. J.; Philips, R. A. *THEOCHEM* **1985**, *123*, 291.
(16) Liebermann, H.-P.; Buenker, R. J. *Revised version of the MRD-CI computer programs*; University of Wuppertal: Wuppertal, Germany, 2006.
(17) Pacios, L. F.; Christiansen, P. A. *J. Chem. Phys.* **1985**, *82*, 2664.
(18) Dunning, T. H., Jr. *J. Chem. Phys.* **1989**, *90*, 1007.
(19) Woon, D. E.; Dunning, T. H., Jr. *J. Chem. Phys.* **1994**, *100*, 2975.
(20) Davidson, E. R. In *The World of Quantum Chemistry*; Daudel, R., Pullman, B., Eds.; Reidel: Dordrecht, 1974; p 17.
(21) Hirsch, G.; Bruna, P. J.; Peyerimhoff, S. D.; Buenker, R. J. *Chem. Phys. Lett.* **1977**, *52*, 442.
(22) Patil, S. H.; Tang, K. T.; Toennies, J. P. *Chem. Phys. Lett.* **2002**, *364*, 371.
(23) Keil, M.; Danielson, L. J.; Buck, U.; Schleusener, J.; Huisken, F.; Dingle, T. W. *J. Chem. Phys.* **1988**, *89*, 2866.
(24) Devdariani, A. Z.; Zagrebin, A. L. *Khim. Fiz.* **1985**, *4* (4), 445; English translation in *Sov. J. Chem. Phys. (GB)* **1987**, *4* (4), 722.
(25) Devdariani, A. Z.; Zagrebin, A. L. *Khim. Fiz.* **1985**, *4* (6), 739; English translation in *Sov. J. Chem. Phys. (GB)* **1987**, *4* (12), 1201.
(26) Devdariani, A. Z.; Zagrebin, A. L.; Blagoev, K. B. *Ann. Phys. Fr.* **1989**, *14* (5), 467.
(27) Zagrebin, A. L.; Tserkovnii, S. I. *Opt. Spectrosc.* **1995**, *79* (4), 556.